Arch. Metall. Mater., Vol. 61 (2016), No 3, p. 1613–1622

DOI: 10.1515/amm-2016-0263

P. KULECKI*, E. LICHAŃSKA*, A. RADZISZEWSKA*, M. SUŁOWSKI*,#

FRACTOGRAPHY AND POROSITY ANALYSIS OF Cr AND Cr-Mo PM STEELS

The aim of the study was to evaluate the effect of processing variables on the porosity and fractography of Cr and Cr-Mo PM steels. The measurements were performed on sintered steels made from commercial Höganäs pre-alloyed powders: Astaloy CrA, Astaloy CrL and Astaloy CrM with two different carbon concentrations (0.2% and 0.6%) added in the form of ultra fine graphite powder grade C-UF. Following mixing in Turbula mixer for 30 minutes, green compacts were single-action pressed at 660 MPa according to PN-EN ISO 2740 standard. Sintering was carried out in a laboratory horizontal tube furnace at 1120°C and 1250°C for 60 minutes, in an atmosphere containing 5%H_2 and 95%N_2. After sintering, the samples were tempered at 200°C for 60 minutes in air. For porosity evaluation computer software was employed. Hitachi S-3500M SEM equipped with EDS (made by Noran) was employed for fracture analysis. The steel based on Astaloy CrM pre-alloyed powder is characterized by fine pores and good mechanical properties. When sintered at 1250°C, it had area of pores approx. 7.12 μm^2, ultimate tensile strength (UTS) about 679 MPa and elongation about 4%. The steels were characterized by ductile/cleavage and ductile fractures.

Keywords: sintered steels, alloying elements, porosity, fractography, mechanical properties

1. Introduction

Sintered materials have porous character of structure with the porosity depending on the final sintering conditions. Porosity can be a desirable feature for specific products, such as filters or oil-less bearings [1-2]. For example, filters based on PM steel are characterized by total porosity up to 35%. During sintering, particles of powder are bound, pores can be spheroidized and consequently mechanical properties improved [1]. Porosity of sintered parts can be controlled in a wide range by: powder processing, pressing pressure, sintering temperature, sintering time, sintering atmosphere, chemical composition and additional processing [3-6]. During sintering, the parameters which influence the porosity of the material include: surface grain boundary and volume diffusion and also evaporation and condensation of metal vapours. Atomic diffusion causes particle bonding and decreases porosity. Increasing the sintering temperature increases the velocity of atomic diffusion.

There are several methods of porosity measurement: determination of apparent density, light microscopy, SEM, capillary condensation, mercury porosimetry and small angle x-ray scattering. The results of these measurements are usually total volume of pores, shape, equivalent circular diameter [7].

Tests of mechanical properties (e.g. tensile tests, bending tests) reveal fracture surfaces of specimens. After these tests, the failure can be determined by studying the characteristics of the fracture surface. The fracture also gives information on the macroscopic scale about brittle or ductile character of failure [8-11]. Using light microscopy technique, the failure in metals can be classified according to loading mode (overload, fatigue, creep), amount of plastic deformation involved in failure and fracture micromechanism operating during monotonically increasing force [11]. Regarding the fracture path, the basic types of fracture processes, from material and physical aspects, are ductile, brittle and fatigue fracture, stress corrosion fracture and creep fracture [11]. Investigations of failures are carried out by SEM at high magnification, which enables observation of crack "nucleus" e.g. oxides, notches, foreign inclusions, nitrides, twins, grain boundaries and voids [8-10]. The morphology of the fracture surface is the source of information about the relationship between the microstructure and material properties, as well as the cause of early failure of the component and it is the result of individually acting fracture mechanisms. All these depend on the local stress state, local stress direction, temperature, microstructure, loading rate [11].

2. Experimental procedures

The powders used in investigations were pre-alloyed iron powders: Astaloy CrL, Astaloy CrM and Astaloy CrA. Carbon, in the form of graphite C-UF (ultra fine), in amounts of 0.2% and 0.6%, was introduced into the mix. The powder mixture were prepared in a Turbula mixer for 30 min.

The mixed powders were single-action pressed at pressure 660 MPa according to PN-EN ISO 2740 standard.

* AGH UNIVERSITY OF SCIENCE AND TECHNOLOGY, FACULTY OF METALS ENGINEERING AND INDUSTRIAL COMPUTER SCIENCE, AL. MICKIEWICZA 30, 30-059 KRAKÓW, POLAND

Corresponding author: sulek@agh.edu.pl

Sintering was carried out using a tube furnace in a semi-closed container at 1120°C and 1250°C for 60 minutes in a mixture of hydrogen and nitrogen (the ratio 5:95) with a dew point of -60°C. The heating and cooling rates were 75°C/min and 60°C/min, respectively. After sintering, the samples were tempered at 200°C for 60 minutes in air, and then mechanically tested. Also microstructure and fracture investigation took place. Table 1 presents chemical compositions of the examined steels.

TABLE 1

Chemical compositions of investigated steels

Chemical composition	Designation
Fe+1.8%Cr+0.2%C	CrA+0.2%C
Fe+1.8%Cr+0.6%C	CrA+0.6%C
Fe+1.5%Cr+0.2%Mo+0.2%C	CrL+0.2%C
Fe+1.5%Cr+0.2%Mo +0.6%C	CrL+0.6%C
Fe+3%Cr+0.5%Mo+0.2%C	CrM+0.2%C
Fe+3%Cr+0.5%Mo+0.6%C	CrM+0.6%C

The following tests were carried out:

- porosity measurement,
- analysis of fractures.

Procedure of preparing of metallographic sections was described in Ref. [12]. Metallographic investigations were carried out using Leica DM4000M optical microscope (bright field (BF)) at magnification 100x on cross-sections of steel samples perpendicular to the tensile direction. Porosity analysis was carried out using the SigmaScan Pro v. 4.0 computer program. To analyze porosity statistically, photographs of unetched cross-sections, e.g. Fig. 1, were used.

Statistical analysis of porosity was conducted according to Ref. [13]. During porosity measurements the following parameters: Perimeter, Area and Feret diameter were taken into account. For accurate measurement of porosity, it is important to set the parameter Threshold; for these analyses the value Threshold was 100. Table 2 presents definition and description of selected parameters from SigmaScan Pro computer program.

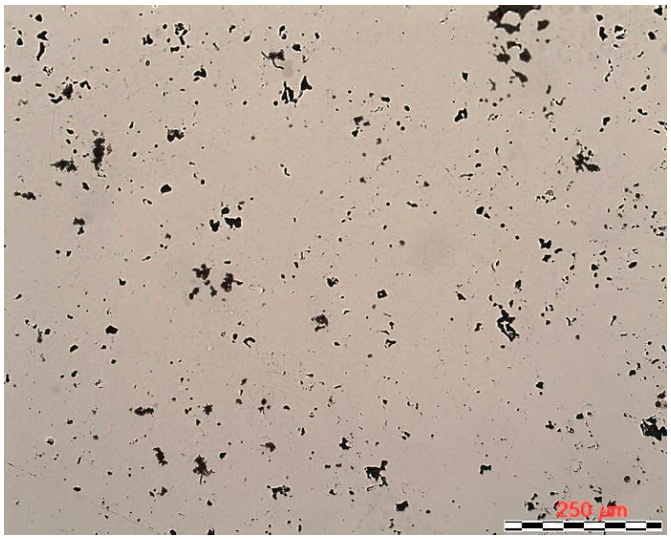

Fig. 1. Microstructure of Astaloy CrA+0.6% C PM steels sintered at 1250°C (unetched)

TABLE 2

Definition and description of parameters analysed using SigmaScan Pro computer program [13]

Description of parameters	Name of parameter
Perimeter of analyzed pore	Perimeter
Area of measured pore defined by amount of pixels which comprise the object	Area
Diameter of fictive circle with the same area as the measured pore. This area is given by $\sqrt{\frac{4S}{\pi}}$	Feret diameter

S- area of pore from micrographs

Fracture investigations were carried out using Hitachi S-3500M SEM equipped with EDS (made by Noran). Fractures of PM Cr and Cr-Mo steels were observed with magnifications 500x, 1500x and 3000x.

3. Results of research

Tables 3 and 4 report mechanical properties of sintered steels and show porosity results, respectively. Characteristic fractures of investigated steels are presented in Fig. 2-7.

TABLE 3

The mechanical properties of investigated PM steels – mean values (10 samples) [7]

Designation	1120°C					1250°C				
	UTS MPa	$R_{0.2}$ yield offset, MPa	A, %	TRS, MPa	HV 0.1	UTS MPa	$R_{0.2}$ yield offset, MPa	A, %	TRS, MPa	HV 0.1
CrA+0.2%C	336±19	198±17	5.41±0.83	506±55	125±22	319±45	221±33	8.22±0.53	547±24	117±17
CrA+0.6%C	525±21	257±8	3.12±0.28	838±54	201±62	717±39	308±21	2.83±2.72	1134±73	223±62
CrL+0.2%C	355±6	202±7	4.40±0.47	485±36	133±32	372±5	258±7	5.31±0.89	517±27	126±24
CrL+0.6%C	565±20	285±13	1.31±0.27	981±24	182±47	629±20	291±29	2.66±0.96	1082±36	221±44
CrM+0.2%C	700±23	401±72	2.41±0.77	959±31	210±42	679±46	329±37	4.03±0.72	998±65	227±65
CrM+0.6%C	818±88	294±20	1.35±0.87	1206±83	379±89	870±33	312±14	2.70±0.94	1392±144	320±78

TABLE 5

The mean values and standard deviations of Perimeter, Area, Feret diameter and amount of pores for PM steels based on Astaloy CrA, Astaloy CrL, Astaloy CrM with 0.2% C and 0.6%C sintered at 1120°C and 1250°C (10 samples)

Designation	1120°C				1250°C			
	Perimeter, μm	Area, μm^2	Feret diameter, μm	Amount of pores	Perimeter, μm	Area, μm^2	Feret diameter, μm	Amount of pores
CrA+0.2%C	9.49±28	9.62±65	2.45±2	1883	10.38±36	11.71±80	2.57±3	881
CrA+0.6%C	11.05±26	13.29±66	2.93±3	2466	10.80±37	12.48±73	2.65±3	2261
CrL+0.2%C	7.88±25	6.66±55	2.13±2	2295	8.82±34	8.71±75	2.24±2	1287
CrL+0.6%C	10.66±27	11.67±63	2.75±3	2572	10.50±30	11.82±68	2.67±3	2063
CrM+0.2%C	10.06±28	9.45±59	2.58±2	1837	8.37±26	7.12±53	2.20±2	2272
CrM+0.6%C	12.72±27	16.55±65	3.30±3	2113	13.15±32	18.54±80	3.38±3	1508

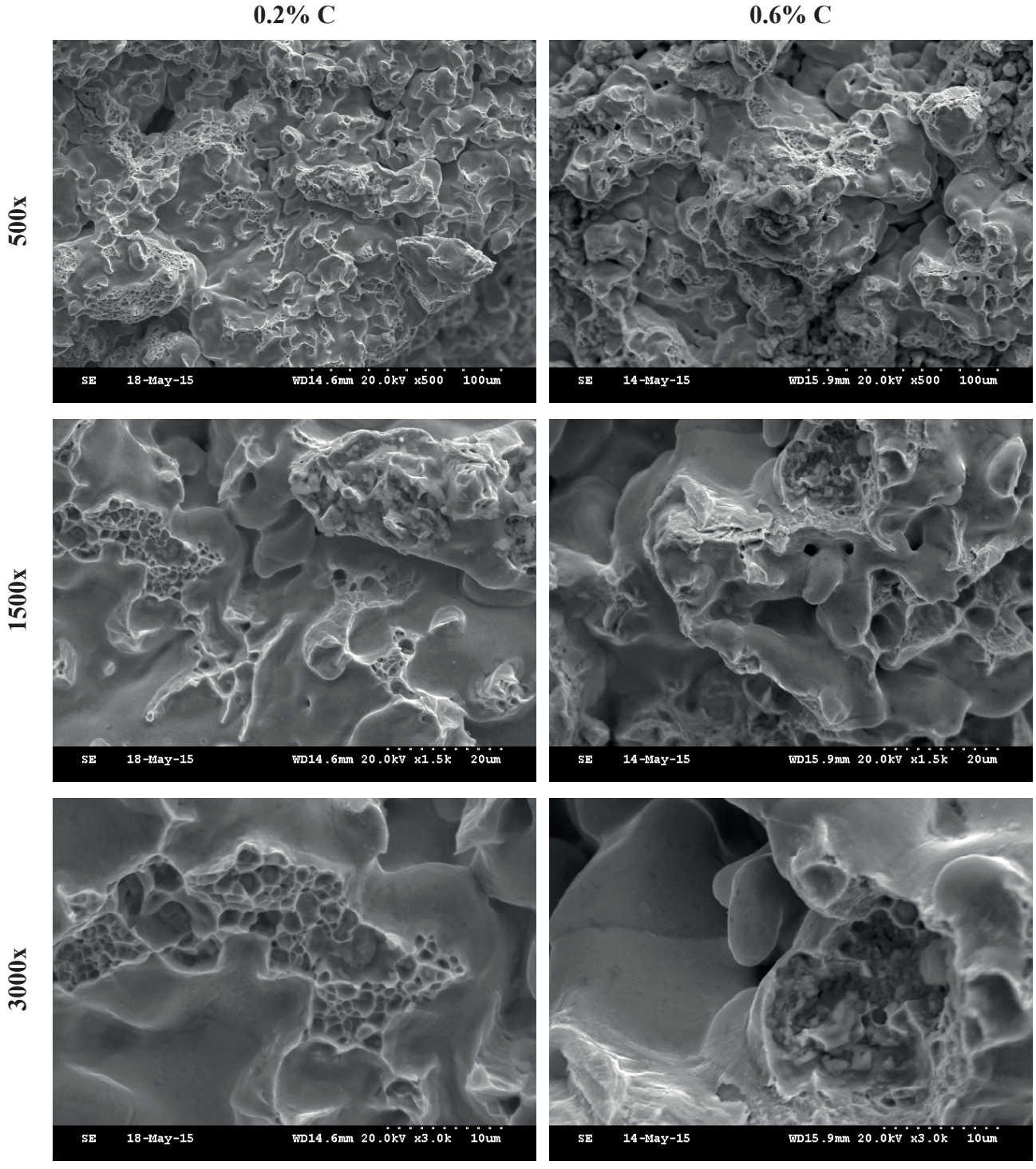

Fig. 2. The fracture of PM steels based on pre-alloyed Astaloy CrA powder, sintered at 1120°C (SEM)

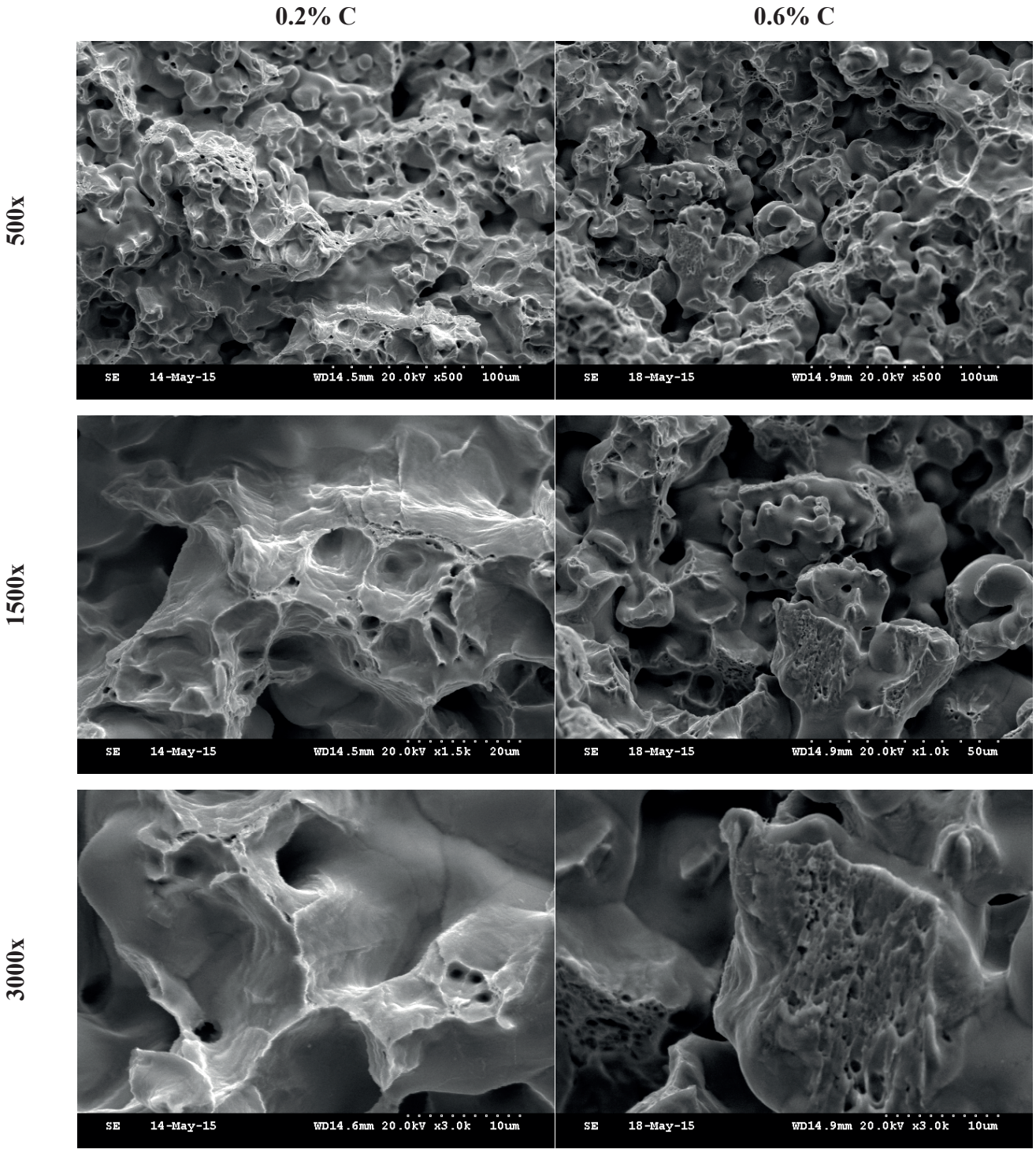

Fig. 3. The fracture of PM steels based on pre-alloyed Astaloy CrA powder, sintered at 1250°C (SEM)

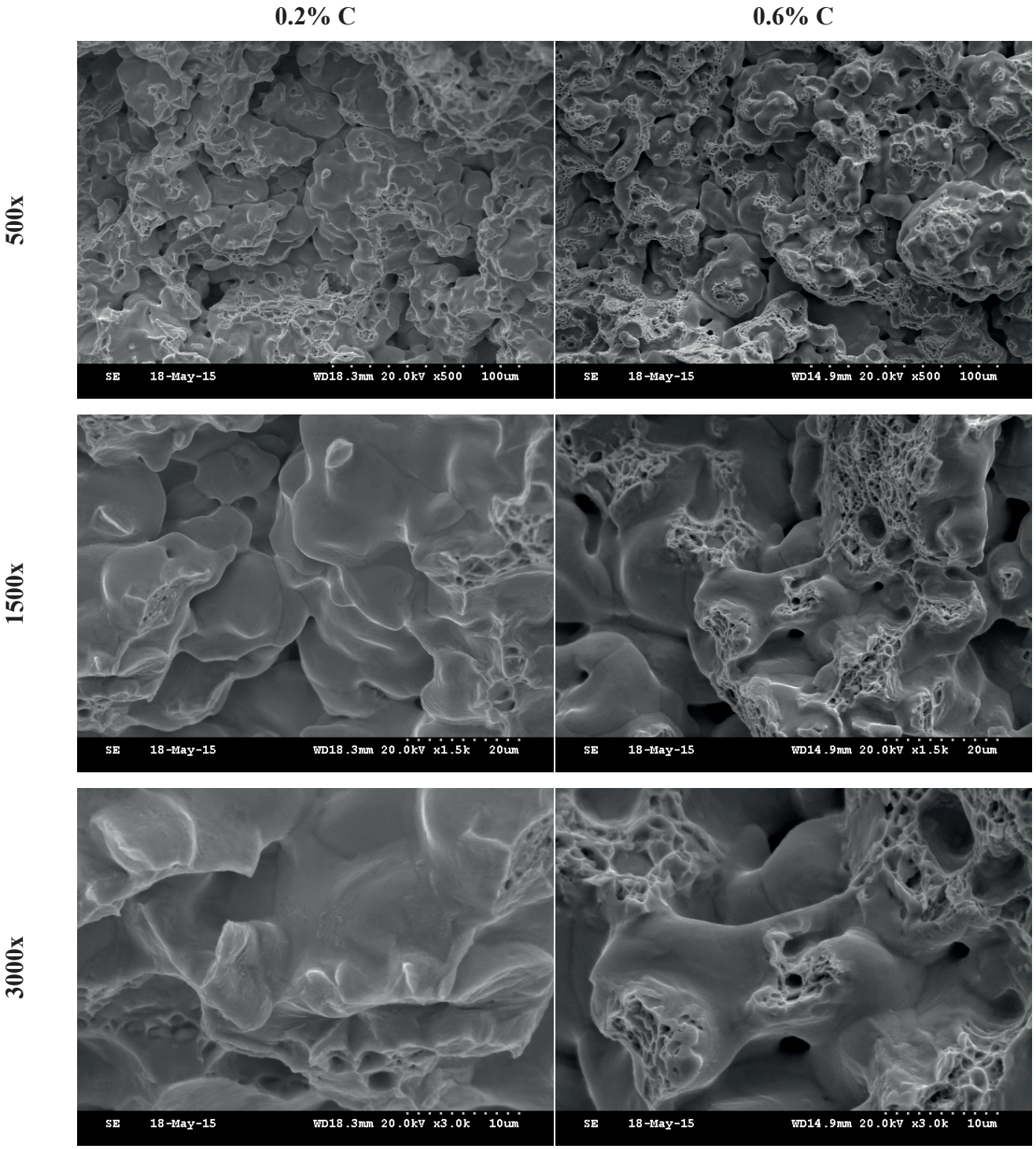

Fig. 4. The fracture of PM steels based on pre-alloyed Astaloy CrL powder, sintered at 1120°C (SEM)

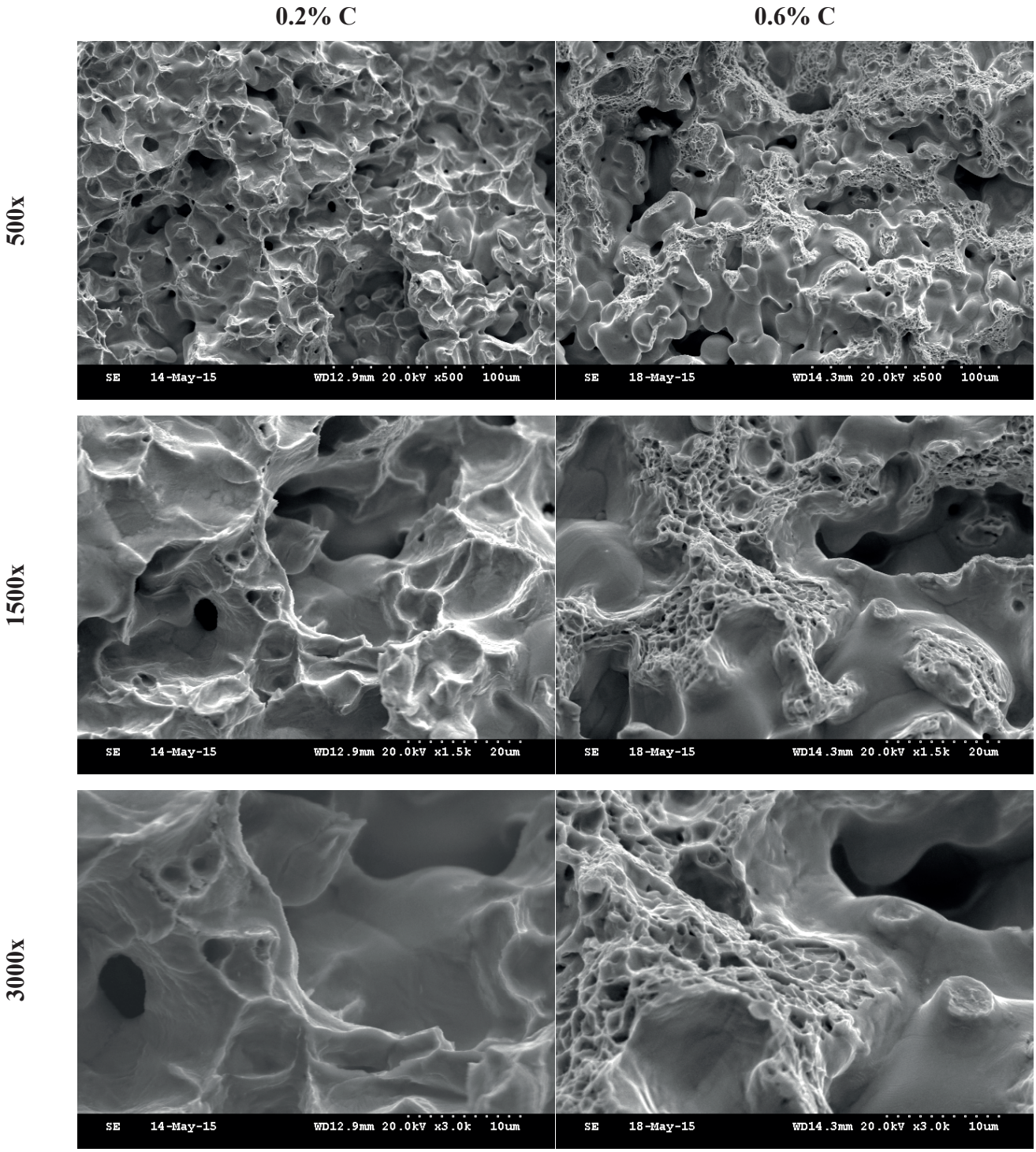

Fig. 5. The fracture of PM steels based on pre-alloyed Astaloy CrL powder, sintered at 1250°C (SEM)

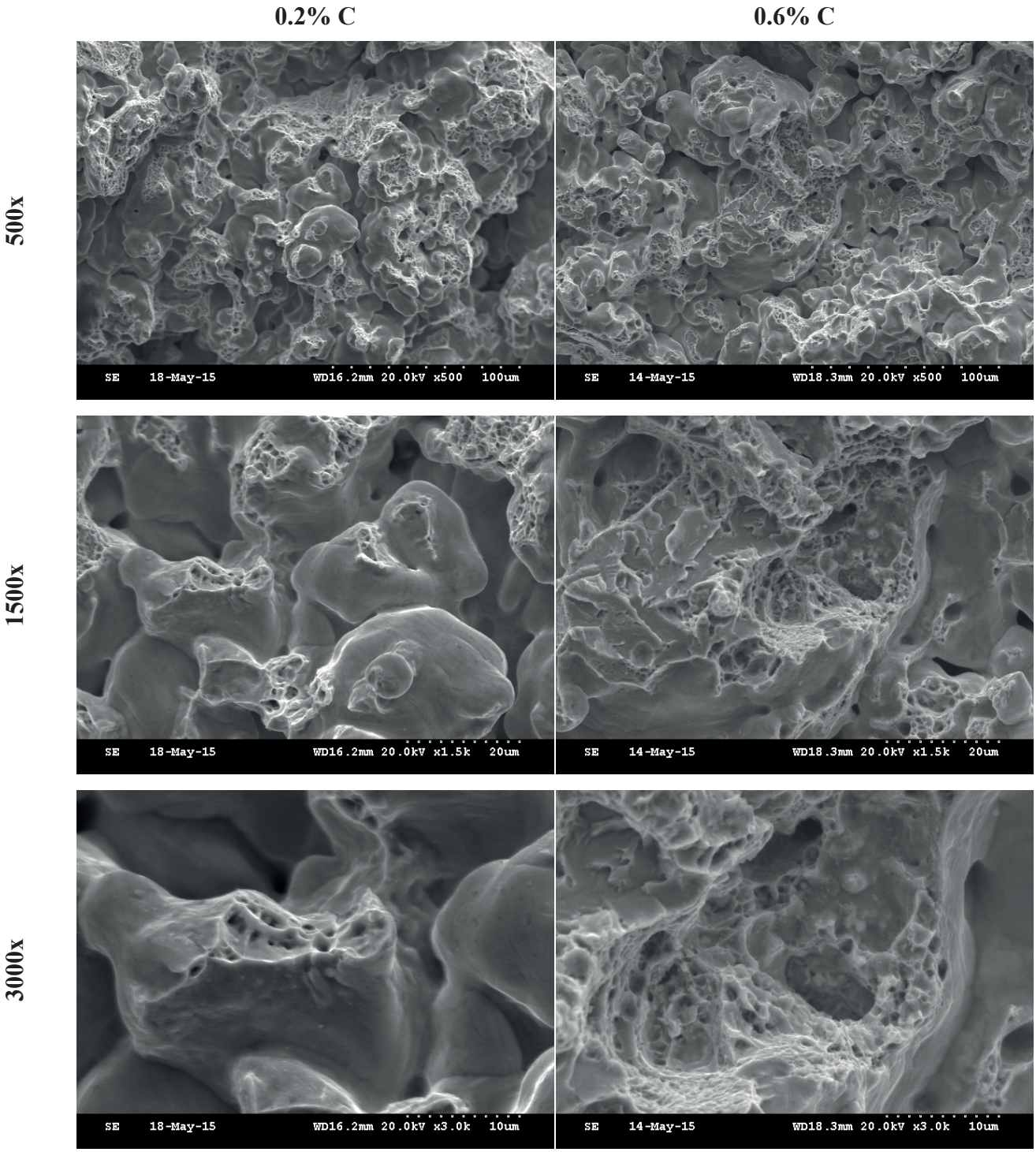

Fig. 6. The fracture of PM steels based on pre-alloyed Astaloy CrM powder, sintered at 1120°C (SEM)

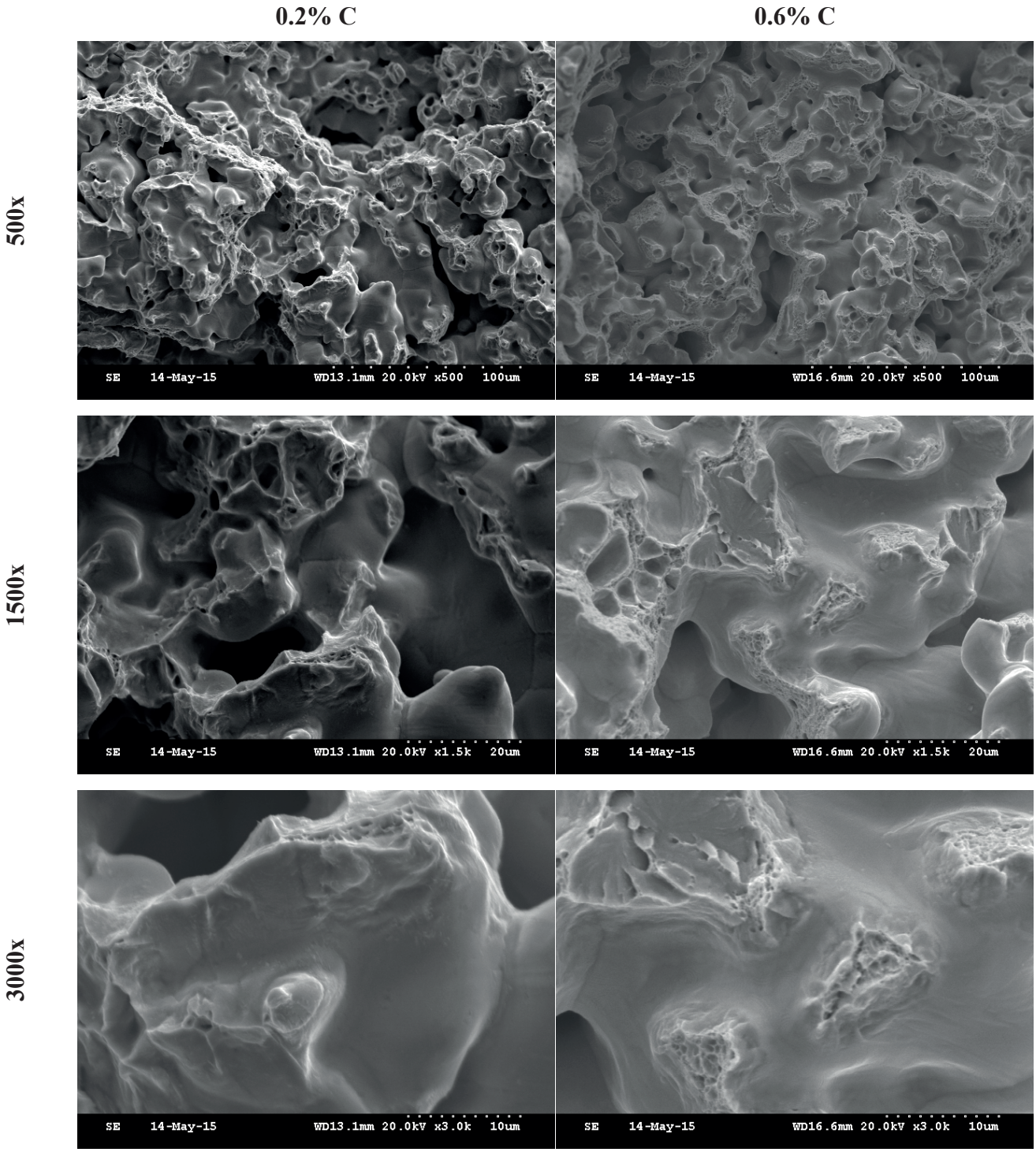

Fig. 7. The fracture of PM steels based on pre-alloyed Astaloy CrM powder, sintered at 1250°C (SEM)

4. Discussion of results

After sintering at 1250°C, steel based on Astaloy CrA+0.2%C was characterized by a slightly higher area of pores in comparison with samples sintered at 1120°C. In this case, after higher sintering temperature, total amount of pores significantly decreased from 1883 to 881. Material based on Astaloy CrA+0.2%C, sintered at 1250°C is characterized by the lowest total amount of pores in comparison with all investigated variants. It's connected with the lowest concentration of alloying additions, high plasticity of Astaloy CrA powder, suitable sintering temperature (1250°C) and low amount of carbon (0.2%C). Steel based on Astaloy CrA+0.6%C sintered at higher temperature revealed decreasing dimensions of pores. These results are related to mechanical properties presented in Table 3.

For steel based on Astaloy CrL+0.2%C sintered at the higher temperature, increased values of porosity parameters (Table 2) were observed. Total amount of pores slightly decreased at the higher sintering temperature. This steel after sintering at 1120°C was characterized by the lowest parameters - Perimeter, Area and Feret diameter, in comparison with all

investigated steels. The lowest values of parameters (Table 2) are connected with good technological properties of Astaloy CrL powder – its good compressibility and plasticity and also matched accurate sintering conditions. Porosity parameters (Perimeter, Area, Feret diameter) were similar for both sintering temperatures for the Astaloy CrL+0.6% C variant.

When sintering temperature was increased, for steel based on Astaloy CrM+0.2%C, porosity parameters described in Table 2 (Perimeter, Area and Feret diameter) were lower in comparison with those recorded after sintering at 1120°C. In this case, the total amount of pores increased from 1837 to 2272. Steel based on Astaloy CrM+0.2%C sintered at 1250°C was characterized by the lowest porosity parameters (Perimeter, Area and Feret diameter), which caused its good mechanical properties. It is connected with the highest content of alloying additions, as compared to Astaloy CrA and Astaloy CrL powders. Steel based on Astaloy CrM+0.6%C sintered at the higher temperature was characterized by the biggest areas of pores in comparison with all investigated variants. Simultaneously, with increasing sintering temperature up to 1250°C, total amount of pores decreased from 2113 to 1508.

Higher carbon content in all variants caused increased size of pores. During sintering, higher amounts of carbides were created. These carbides blocked diffusion processes, causing slower shrinkage of the pores. The best mechanical properties and the lowest porosity were obtained for steel based on Astaloy CrM with addition of 0.2% C, sintered at 1250°C.

Fig. 2 shows fractures of steel based on Astaloy CrA+0.2%C, which revealed ductile fracture. This steel was characterized by low hardness 117-125 HV 0.1. After sintering at 1120°C, oxide segregation was observed, in contrast to high temperature sintered steel, in which segregation was not detected. In steels based on Astaloy CrA+0.6%C failures were mixed, but mostly with quasi-cleavage areas. Hardness of this steel was higher in comparison to steel based on Astaloy CrA+0.2%C, being 201-223 HV 0.1. After sintering at 1120°C oxide segregation was observed, but after increasing the sintering temperature to 1250°C, there was no segregation.

Failure of steels based on Astaloy CrL+0.2%C were characterized by ductile areas and after sintering at 1250°C necks were bigger, which testifies good bonding between particles, which is connected with the increase of elongation from 4.44% to 5.31%. The character of failures in steels based on Astaloy CrL+0.6%C was both ductile and brittle. Steels sintered at 1250°C were characterized by better connections between particles and higher elongation of 2.66%, in comparison with steels sintered at 1120°C (A = 1.31%).

Fractography of steels based on Astaloy CrM+0.2%C revealed ductile fractures, which is related with elongation in the range 2.41% - 4.03%. In steel sintered at 1120°C, oxide segregation was observed, but in steel sintered at the higher temperature segregation was not observed. After sintering at the higher temperature, necks were bigger and longer, because the higher sintering temperature caused better bonds between the particles. Lower content of carbon caused lower toughness (210 – 227 HV 0.1) in comparison with steel based on Astaloy CrM+0.6%C.

Increase the carbon content up to 0.6%C in steels based on Astaloy CrM caused changes in the character of the failure - to more brittle. The analysis of failures of this steel revealed more cleavage areas, especially after sintering at 1120°C. With increasing carbon content, the steel had a higher hardness (320 – 379 HV 0.1) and was more brittle.

Higher sintering temperature caused oxide reduction, better connections between particles and better plasticity. Increasing carbon content caused reduction of neck size and lower plastic properties in all alloy variants.

5. Conclusions

The studies lead to the following conclusions:

1. Higher carbon content resulted in an increase size of pores for all alloy variants.
2. Steels based on Astaloy CrL+0.2%C and Astaloy CrM+0.2%C sintered at 1120 and 1250°C, respectively, were characterized by the lowest porosity parameters.
3. Steels with the lowest porosity, based on Astaloy CrL+0.2%C and Astaloy CrM+0.2%C sintered at 1120°C and 1250°C, respectively, were characterized by good mechanical and plastic properties.
4. Steel based on Astaloy CrM+0.6%C sintered at 1250°C was characterized by the highest size of pores.
5. Increasing the sintering temperature changed the character of failures to more ductile for all alloy variants.
6. Increasing carbon content caused decreased plasticity, which corresponds to fractographic observations.
7. Most cleavage content in failure areas was observed in steels based on Astaloy CrM.

Acknowledgments

The financial support of the Ministry of Science and Higher Education under AGH contract no 11.11.110.299 is acknowledged.

REFERENCES

[1] R. M. German: Powder metallurgy science, second edition, MPIF, Princeton (1994).
[2] W. Missol: Spiekane Części Maszyn, Wydawnictwo „Śląsk”, Katowice (1976).
[3] T. Pieczonka, M. Sułowski, A. Ciaś, Archives of Metallurgy and Materials, 57, (4), 1001-1009 (2012).
[4] M. Sułowski, A. Ciaś, Archives of Metallurgy and Materials, 54, (4), SI, 1093-1102 (2009).
[5] M. Sułowski, Archives of Metallurgy and Materials, 53, (2), 124-140 (2010).
[6] Ch. Fiał, E. Dudrova, M. Kabatova, M. Kupkova, M. Selecka, M. Sułowski, A. Ciaś, Powder Metallurgy Progress, 15, SI, 124-129 (2015).
[7] J. Lis, SU 1566, AGH Uczelniane Wydawnictwa Naukowo-Dydaktyczne, Kraków (2000).
[8] M. Blicharski, Odkształcanie i pękanie, Wydaw. AGH, Kraków (2002).
[9] K. Przybyłowicz, Strukturalne aspekty odkształcania metali, WNT, Warszawa (2002).
[10] J. W. Wyrzykowski, E. Pleszakow, J. Sieniawski, Odkształcanie

i pękanie metali, WNT, Warszawa (1999).
[11] E. Dudrova, M. Kabatova, Workshop Fractography of Sintered Materials – Principles and Application, IMR SAS Kosice (2015).
[12] P. Kulecki, M. Sułowski, M. Ciesielka, Rudy i Metale Nieżelazne, **5**, (58), 266-272 (2013).
[13] M. Sułowski, Rudy i Metale Nieżelazne **10**, (52), 627–645 (2008).